Realization and performance evaluation of high speed autofocusing for direct laser lithography

Hyug-Gyo Rhee, Dong-Ik Kim, and Yun-Woo Lee

Citation: Review of Scientific Instruments **80**, 073103 (2009); doi: 10.1063/1.3176468
View online: http://dx.doi.org/10.1063/1.3176468
View Table of Contents: http://aip.scitation.org/toc/rsi/80/7
Published by the American Institute of Physics

Realization and performance evaluation of high speed autofocusing for direct laser lithography

Hyug-Gyo Rhee,[1,a)] Dong-Ik Kim,[2] and Yun-Woo Lee[1]
[1]*Space Optics Research Center, Korea Research Institute of Standards and Science, Daejeon 305-340, Republic of Korea*
[2]*Division of Instrument Development, Korea Basic Science Institute, Daejeon 305-333, Republic of Korea*

(Received 11 May 2009; accepted 22 June 2009; published online 15 July 2009)

The autofocusing is one of the important parts in the automated vision inspection or measurement using optical microscopes. Moreover, laser micromachining or laser lithography requires a high speed and precision autofocusing. In this paper, we propose and realize an autofocusing system using two cylindrical lenses, which is the enhanced version of the previous astigmatism method. It shows very good performances, especially very high speed and the largest range in comparison with the previous astigmatic methods. The performance of our autofocusing system was evaluated by tracing the linear stage whose position was monitored by a commercial laser interferometer. Then we applied the autofocusing to the direct laser lithographic system, and successfully fabricated circular symmetry patterns on a 300 mm diameter surface with the resolution of less than 1 μm within the defocusing range of ± 50 μm. The speed of the autofocusing was 150 Hz. © *2009 American Institute of Physics.* [DOI: 10.1063/1.3176468]

I. INTRODUCTION

A direct lithography using a laser,[1–5] which has a noncontact procedure, is superior to electron beam lithography because of relatively low-cost system constitution and fine pattern fabrication in the range from several hundred nanometers to several micrometers in which one has fast and novel performance for a large area substrate. Recently, microfabrication using a high-powered laser is also being increased because the fabrication of a brittle material such as ceramic or glass which is difficult to treat in machining is possible. The most important requirement in the above mentioned laser applications are to control a beam focus to be matched onto a target surface during a fabrication. A constant focal point is very important because a focal position in a vertical direction is directly related to fabricated linewidth, depth, and besides the shape of a cross section. This can be achieved by means of autofocusing control, and uniform result also can be obtained.

In general, there are two different schemes for realizing autofocusing. One is to flexibly vary the focal distance of an objective lens,[6–8] the other is to mechanically shift the objective lens or the substrate itself.[9–13] We have used the latter case so-called active controlling that using an auxiliary light source. The method which we introduce here offers several advantages over existing ones, such as optical triangulation technique, eccentric light method,[12] and confocal scheme.[13] Compared to these, our method can have a good signal-to-noise ratio and large working range by using a couple of cylindrical lenses. Moreover, the method can be applicable up to large scale optical fabrications (up to 400 mm diameter) because of fast focusing speed and very large defocusing range which is distinguish from any other methods. The details of our system are presented in Sec. II. In Sec. III, we show some experimental results.

II. CONSTITUTION OF AUTOFOCUSING SYSTEM

Figure 1 shows the configuration of our laser lithographic system, which includes the intensity stabilization and control part, the writing head including autofocusing mechanism, the stage part, and the alignment part.[5] The system writes fine patterns onto chromium or photoresistor coated substrate with a high magnifying objective lens [Mitutoyo 100×, numerical aperture (NA): 0.7]. Due to the high NA of the objective, in our case, the depth of focus (DOF) is very short (about 0.5 μm for being used wavelength of 488 nm) according to the following equation that is given by

$$\mathrm{DOF} = 0.5\frac{\lambda}{\mathrm{NA}^2}, \tag{1}$$

where λ is the wavelength of the writing source light.[14] For this reason, the need for a real-time precision control of the constant distance between objective lens and a target surface is imperative at all times. It is important to maintain constantly writing beam focus on the all of a surface during a fabrication for producing good quality of computer generated holograms and diffractive optics elements. A principal factor affecting the variation of the focus is the tilted surface of a substrate. Because of the inclination, the size of the focal point is varied during the fabrication. In the result the linewidth is broader and the depth is shallower. In order to correct the defocusing amount which arises from the above reason, we have introduced an astigmatic strategy but enhanced new one, one of the active autofocusing methods, and produced an independent autofocusing controller to overcome speed limitation. The mechanism of the autofocusing system

a)Electronic mail: hrhee@kriss.re.kr.

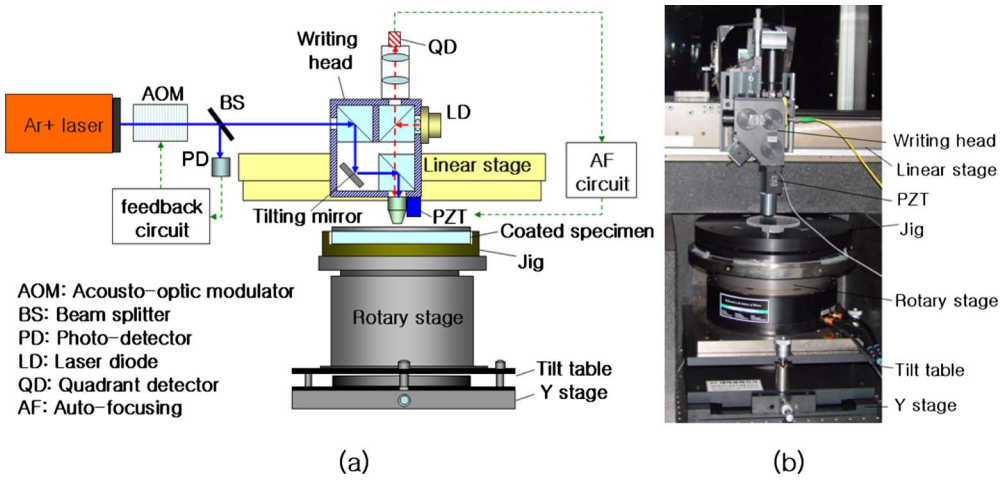

FIG. 1. (Color online) (a) Configuration and (b) photographic views of the laser lithographic system.

is as follows: an auxiliary reflection beam (laser diode) from the surface of a substrate goes through a set of cylindrical lenses, and makes various intensity shapes on the focal plane depending on the distance variation between the surface and the cylindrical lens set. Here, the perpendicular cylindrical lens set plays an important role because it change sharply the intensity shape in the x or y-direction according to the distance, so it maximizes astigmatism that it can increase defocusing amount and sensitivity. To this end, it is possible to make large scale optical fabrication maintaining uniform precision in comparison with the previous astigmatic method[9] which is only applicable to small scale cases such as compact disc (CD)/digital versatile disc (DVD) pickup. The intensity shape variation is accepted by a quadrant detector (EG&G UV140BQ-4) and then introduced to a computer by four different cables. The four signals from the quadrant detector (QD) make an error signal in the computer and feedback the error signal to the piezoelectric transducer (PZT) actuator (PI P-721.0LQ) supported to the micro-objective lens to maintain the constant focal point on the substrate. By doing so, the constant focus can be formed on the surface. However, this method has a speed limitation of 9 Hz—if a spindle rotates one revolution in one second, then the autofocusing operates one time every 40°—so that it is impossible to control the autofocusing on the high speed rotation with more than the angular velocity of 360 deg/s. To improve the limitation, we have made an autofocusing controller built-in an electronic circuitry independent of the computer. The details of our system are explained as Secs. II A and II B.

A. Optical system

Depending on the laser diode beam shape reflected from a target surface through an optical system, QD makes different photocurrents at four detecting areas for the autofocusing. Figure 2 shows the optical system. First, we attached a bandpass filter, a linear polarizer, a biconvex lens, and a cube beam splitter to the writing head. The role of each part is as follows: the bandpass filter passes only 635 nm laser diode beam except for the 488 and 457.9 nm writing beam. The linear polarizer plays a role of reducing the residue reflection beam in the writing head that acts as a noise source on QD. The biconvex lens adjusts suitably beam scaling on QD and the optical distance from the target surface to QD, and the cube beam splitter reflects off most laser diode beam (about 90%) coming from the surface to the cylindrical lens assembly. The other beam from the beam splitter (about 10%) is monitored by a charge coupled device (CCD). Second, we installed the cylindrical lens assembly composed of two cylindrical lenses right angle to each other on the linear stage. Lastly, QD mounted on a *XYZ* translator was also set up on the stage. In Fig. 2, the beam reflected from the material surface goes although the series of optics and makes a particular spot pattern near the focal planes. The QD is placed between two astigmatic foci that two cylindrical lenses originally have, namely, at the location where the intensity pattern looks to be a perfect circle as shown in Fig. 2 (position 2). The orientation of QD lines should be 45° or 135° with respect to the tangential plane of the cylindrical lenses. If the distance between the material surface and the objective is changed, the intensity patterns on QD will also be changed, thereby bringing about the error signal change. The radius of

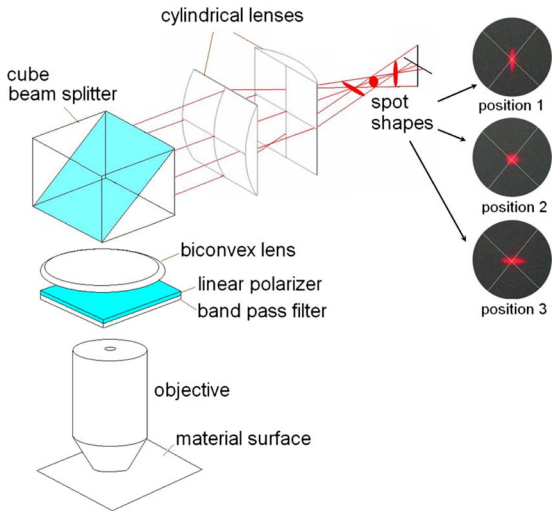

FIG. 2. (Color online) Optical components to generate the autofocusing error signal. The three different kinds of spot shape are formed on the QD according to the distance between the objective and the material surface. Position 2 indicates the exact focal point.

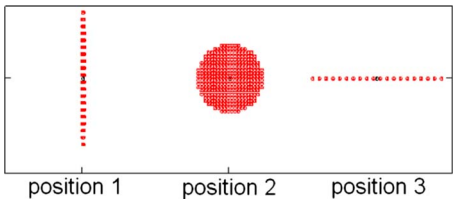

FIG. 3. (Color online) Designed spot diagram at the focal positions. Commercial software for optics design was used for this simulation.

curvature of each cylindrical lens was 15.5 mm, the focal length was 30 mm, the space between two lenses was 5.7 mm, and the effective focal length of two lenses was 15.7 mm. We designed these parameters to maximize the sharpness of the spots at positions 1 and 3 as shown in Fig. 3.

B. Electronic controller

Figure 4 shows the schematic of the electronic controller. Unlike computer calculation for making the error signal, this controller is possible to achieve the high speed autofocusing control up to 150 Hz (PZT modulation limit). Each signal received by QD is guided into the controller through four different BNC cables. In the controller, first, the guided current signals are converted into the voltage signals by current to voltage converters. In this process, the capacitance of a condenser affect considerably to the response time of the PZT actuator. Figure 5 shows Bode diagram according to the capacitance change in which the reducer the capacitance, the faster the actuator response. The optimal capacitance we found here is 1 nF as shown in Fig. 5(c). When the capacitance was less than this, the actuator was overshot even to the minimum gain in our experiment. Especially if no condenser was used like in Fig. 5(d), a lot of noise was occurred in the process of current to voltage conversion. Under the larger capacitance such as Fig. 5(a), the autofocusing speed could not catch up with the rotation speed of 360 deg/s. Next, the converted voltage signals undergo a series of calculation (addition and subtraction), then makes a normalized error signal $e_N(I)$ as shown in the following Eq. (2).

$$e_N(I) = \frac{I_a + I_d - (I_b + I_c)}{I_a + I_d + (I_b + I_c)}, \tag{2}$$

where a, b, c, and d indicate the four sections of QD as shown in the Fig. 6(b), respectively. This normalization is able to reduce noise arising from the sudden light intensity fluctuation caused by dusts and/or stains on the surface of the substrate.[10] In other words, this sudden intensity variation degrades the autofocusing function because of acting as a noise source. The normalized error $e_N(I)$ is divided into three parts and applied proportional integral derivative control to

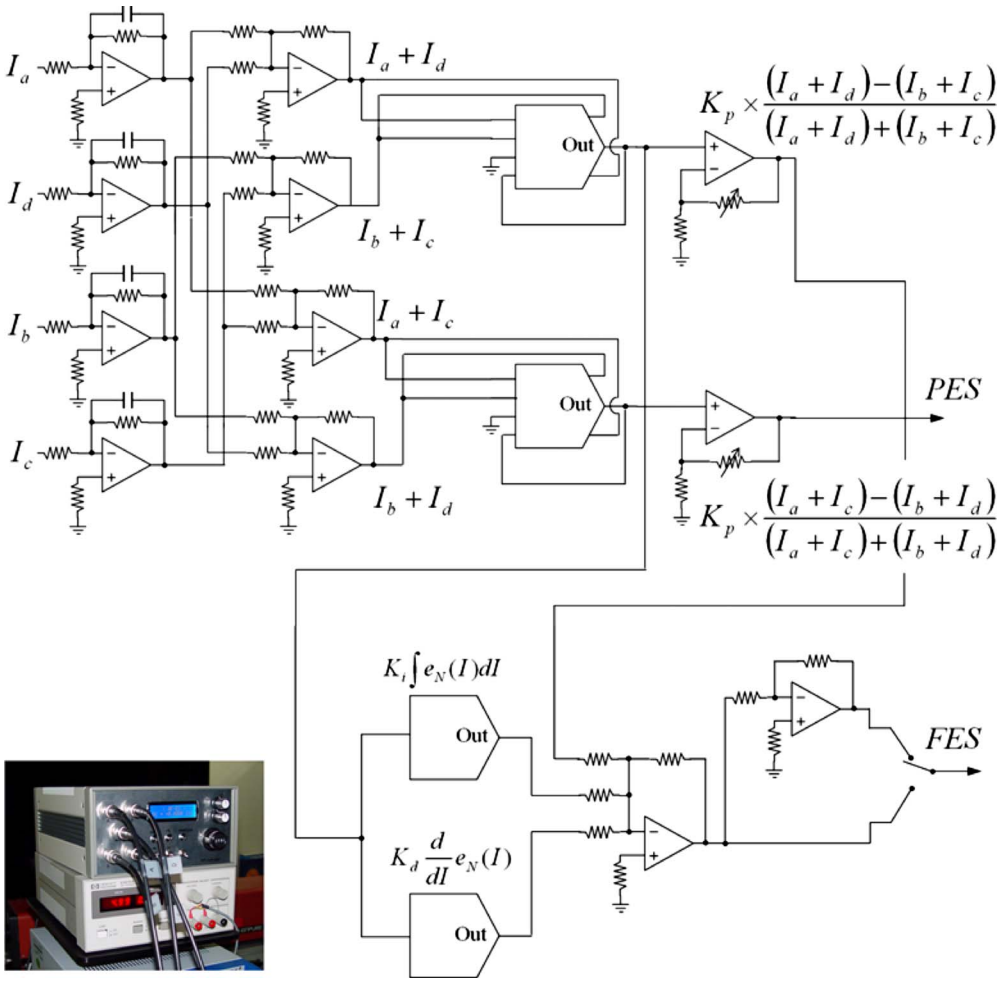

FIG. 4. (Color online) Photographic view of the autofocusing controller and schematic of its circuitry.

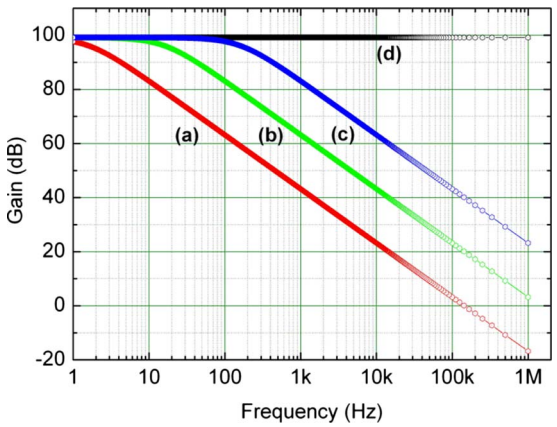

FIG. 5. (Color online) Bode diagram about current to voltage conversion. (a) and (b) are the capacitance of 100 and 10 nF. (c) is in the case of optimal capacitance of 1 nF for fast response of the PZT actuator. (d) shows no condenser case.

each part. Multiplying suitable gains and summing each part, then a final focusing error signal (FES) is made. It can be written as

$$\mathrm{FES} = K_p \times e_N(I) + K_i \times \int e_N(I)dI + K_d \times \frac{de_N(I)}{dI}, \quad (3)$$

where K_p, K_i, and K_d are the proportional, integral, and derivative gain, respectively. We have gotten better result than the case in which the proportional gain was only given. By doing so, residual error after the autofocusing was reduced more (less than 1 μm) and besides the control range was extended twice from ± 25 to ± 50 μm. Now, the remainder of work is to locate the laser beam shape to the center of QD. One problem is that when we look for the zero point for the autofocusing, the error signal would be zero even in the case of Fig. 6(b). To correct this we added a circuit which calculates position error signal (PES) to the controller. PES is given by

$$e_{\mathrm{NP}}(I) = \frac{I_a + I_c - (I_b + I_d)}{I_a + I_c + (I_b + I_d)}, \quad (4)$$

$$\mathrm{PES} = K_p \times e_{\mathrm{NP}}(I), \quad (5)$$

where $e_{\mathrm{NP}}(I)$ represents a normalized error signal for the estimation of position error deviated from QD center and K_p is the proportional gain. By setting FES and PES to be zero,

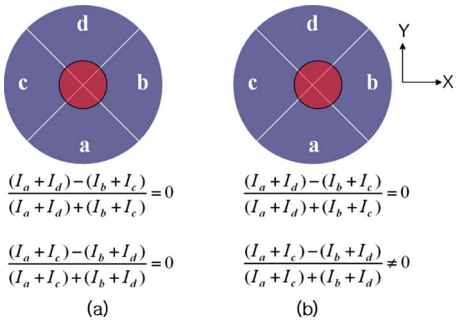

FIG. 6. (Color online) Alignment of QD to find out center at the exact focal point. (a) The exact QD center, (b) a case of off center.

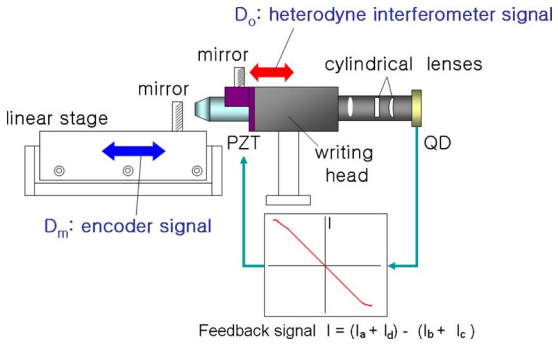

FIG. 7. (Color online) Experimental setup to check the performance of the autofocusing system.

respectively, we can improve the accuracy of our autofocusing control.

III. RESULTS AND DISCUSSION

To find the zero point, QD position with respect to the X and Y axes in Fig. 6 was tuned FES and PES to be 0.000 ± 0.001 V at the initial focal point, and then we turned the control switch on with suitable gains (K_p, K_i, and K_d, respectively). The autofocusing controller gives the error signal to PZT actuator to keep the focusing position during the fabrication. Figure 7 shows a setup to measure the autofocusing error. This configuration was already presented in the reference article,[5] but we tested it again because the autofocusing optics was slightly changed. The mirror attached on the linear stage oscillated, and we measured D_m (the mirror movement) and D_o (the objective movement) at the same time. After whole test, the autofocusing error D_m-D_o was less than 1.1 μm in peak-to-valley value as shown in Fig. 8. When the focusing point moved 1 μm, the line width change in the pattern was approximately 3.6% with 100× objective (NA: 0.7, depth of focus: 0.6 μm). Therefore we suppose that the 1 μm focusing error is allowable. Figure 9 shows CCD snap shots showing the focusing variation on the rotating surface. As shown in Fig. 9(a), the variation of the focus, due to surface tilting (the greatest contribution to the focus variation), according to the rotation angle can be observed. The focus size at 0° is increasing as the substrate

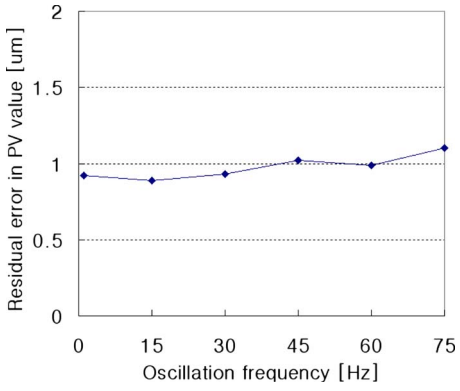

FIG. 8. (Color online) Residual error after the autofocusing. The higher frequency (larger than 75 Hz) test is meaningless because it is over the Nyquist (Ref. 5) sampling limitation (the maximum speed of our PZT actuator is 150 Hz).

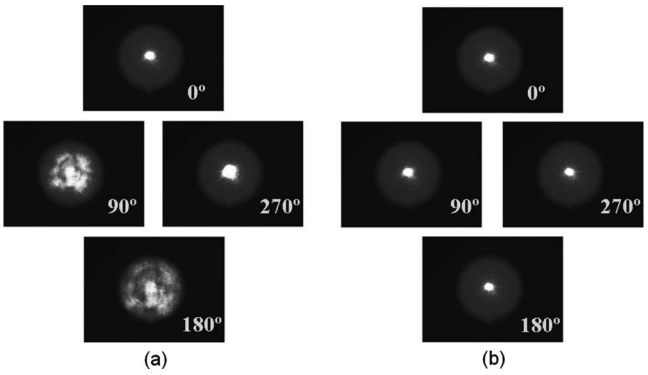

FIG. 9. CCD snapshots of a focal point variation on the rotating substrate (a) before and (b) after the autofocusing control.

rotates, and then back to normal after one rotation. On the contrary, however, once we apply the autofocusing control to it, the focus size is nearly invariant for one rotation. To confirm system performance in detail, we carried out writing tests divided into two parts, that is to say, with and without the autofocusing control. The target glass wafer is coated with chromium of 100 nm thickness. The test writing results given the surface radius change from 4.6 to 14 mm and 10 μm line to line spacing is shown in Fig. 10. As in the inner area of Fig. 10(a), when turn the autofocusing off, the fabricated pattern in the region out of the focus is entirely missed, and what is more, the written areas are also dimming even if the focusing region is little deviated from the focus. Applying the autofocusing control to the whole surface, on the other hand, uniform patterns are well written as shown in the outermost arrowed circle in Fig. 10(a). Even in a small area there is a big difference whether the autofocusing is present or not, to say nothing of a large one. From the comparative results, the significance of autofocusing is emphasized here. Figure 10(b) shows that the patterns on the surface are successfully fabricated to the whole area by means of the autofocusing control. We could also confirm the uniform linewidth of 2.0 μm as shown in Fig. 11 using a commercial white-light scanning interferometer.[15] In addition, we have accomplished the linewidth of 0.6 μm by means of controlling the source laser power. In the light of these facts, we can assure that our autofocusing system is well operated.

IV. CONCLUDING REMARKS

Our direct laser lithographic system can write up to 360 mm diameter substrate coated with chromium or photoresist film. The specific requirements for this are as follows: (a)

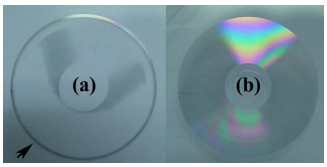

FIG. 10. (Color online) Fabrication results: comparison of (a) before with (b) after the autofocusing control. The arrowed circles in (a) is a result with the autofocusing control to show the significance of it.

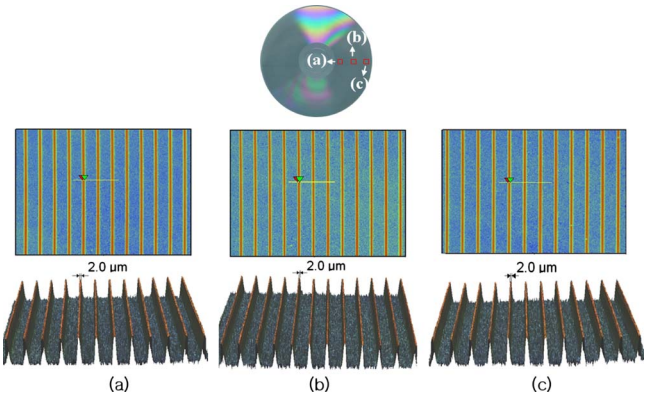

FIG. 11. (Color online) Fabrication results obtained by a commercial white-light scanning interferometer (field of view: 124×93 μm^2, magnification: 50×). Regions (a)–(c) show uniform linewidth of 2.0 μm, respectively.

The range of the autofocusing should cover the whole PZT actuator stroke of 100 μm for a large area fabrication, (b) the spatial uniformity, namely, minimum 0.1 μm linewidth, should be maintained over the whole surface up to maximum diameter of 400 mm. (c) The residual error in peak-to-valley value should be 1 μm below under the high speed rotation of 600 rpm. (d) The autofocusing range should cover ± 50 μm. Unfortunately the previous autofocusing schemes are hard to achieve these requirements. Therefore we proposed and realized a modified autofocusing system using two cylindrical lenses. Our system has high speed and the largest range in comparison with the previous astigmatic methods. In addition, it has a merit that can be applicable to any other purposes, such as the automated vision inspection, the optical microscopes, and the laser micromachining.

ACKNOWLEDGMENTS

We would like to thank Dr. Jae-Bong Song (Korea Research Institute of Standards and Science) for useful discussions. H.-G.R. and D.K. contributed equally to this work.

[1] M. T. Gale, M. Rossi, J. Pedersen, and H. Schutz, Opt. Eng. (Bellingham) **33**, 3556 (1994).
[2] M. Haruna, M. Takahashi, K. Wakahayashi, and H. Nishihara, Appl. Opt. **29**, 5120 (1990).
[3] A. G. Poleshchuk, E. G. Churin, V. P. Koronkevich, V. P. Korolkov, A. A. Kharussov, V. V. Cherkashin, V. P. Kiryanov, A. V. Kiryanov, S. A. Kokarev, and A. G. Verhoglyad, Appl. Opt. **38**, 1295 (1999).
[4] P. Zhou and J. H. Burge, Appl. Opt. **46**, 6572 (2007).
[5] H. Rhee, D. Kim, S. Hong, and Y. Lee, Rev. Sci. Instrum. **79**, 103103 (2008).
[6] L. Zhu, P. C. Sun, and Y. Fainman, Appl. Opt. **38**, 5350 (1999).
[7] Y. Takaki and H. Ohzu, Opt. Commun. **126**, 123 (1996).
[8] A. Kaplan, N. Friedman, and N. Davidson, Opt. Lett. **26**, 1078 (2001).
[9] D. K. Cohen, W. H. Gee, M. Ludeke, and J. Lewkowicz, Appl. Opt. **23**, 565 (1984).
[10] K. C. Fan, C. L. Chu, and J. I. Mou, Meas. Sci. Technol. **12**, 2137 (2001).
[11] M. Forrer, M. Frenz, A. D. Zweig, V. Romano, H. P. Weber, and J. Ochsenbein, Appl. Opt. **30**, 1480 (1991).
[12] Q. Li, L. Bai, S. Xue, and L. Chen, Opt. Eng. (Bellingham) **41**, 1289 (2002).
[13] R. Juskaitis, N. P. Rea, and T. Wilson, Appl. Opt. **33**, 578 (1994).
[14] M. Born and E. Wolf, *Principles of Optics*, 6th ed. (Pergamon, New York, 1983), pp. 370–458.
[15] A. Harasaki, J. Schmit, and J. C. Wyant, Appl. Opt. **39**, 2107 (2000).